Comparison of the energy and mass characteristics of the ^{239}Pu(n_{th},f) and the ^{240}Pu(sf) fragments

C. Wagemans,* E. Allaert, A. Deruytter, R. Barthélémy, and P. Schillebeeckx*
Commission of the European Communities, Joint Research Center, Geel Establishment, Central Bureau for Nuclear Measurements, B-2440 Geel, Belgium
and Studiecentrum voorkernenergie-centre d'Etudes, Nucléaires, B-2400 Mol, Belgium
(Received 14 February 1984)

The energy and mass distributions and their correlations have been studied for the spontaneous fission of ^{240}Pu and the thermal neutron induced fission of ^{239}Pu. A comparison of the ^{240}Pu(sf) and the ^{239}Pu(n_{th},f) results shows a narrower mass distribution, a much higher peak yield, a much lower symmetric fission yield, and a more pronounced fine structure for the spontaneous fission than for the neutron induced fission. The average total kinetic energy is 1.3 MeV higher for ^{240}Pu(sf) than for ^{239}Pu(n_{th},f), and also the energy-mass correlations behave differently in both cases. All these results are discussed and interpreted in the framework of the scission point model of Wilkins *et al.* Finally, the damping of the ^{240}Pu fission mode below the barrier is demonstrated.

I. INTRODUCTION

The characteristics of the mass and energy distributions of the fission fragments emitted during the spontaneous fission of ^{240}Pu are a controversial problem in the fission physics field. Indeed, since 1958 several comparative measurements of the ^{239}Pu(n_{th},f) and the ^{240}Pu(sf) reactions have been performed yielding quite discrepant results[1–7] for both the energy and the mass characteristics. The most striking observation was that three of these experiments yielded a higher total fission fragment kinetic energy for ^{240}Pu(sf) than for ^{239}Pu(n_{th},f) despite the 6.5 MeV more excitation energy available in the latter case. Also for the ^{240}Pu(sf) fragments, mass distribution results strongly different from those of ^{239}Pu(n_{th},f) were reported by some of the authors referred to above.

This controversial situation is a serious handicap for a coherent interpretation of the large variety of experimental studies of the fissioning system ^{240}Pu at various excitation energies [e.g., via ^{240}Pu(γ,f), ^{239}Pu(n,f), ^{239}Pu(d,pf), ..., reactions], from which a better knowledge of the fission dynamics is likely to be deduced. A typical example in this respect is the work of Lachkar *et al.*[8]

In view of the above considerations, a special effort was made, from the experimental as well as from the sample preparation side, to put an end to this puzzling situation. So a new series of measurements was performed in the framework of a collaboration between the Central Bureau for Nuclear Measurements (CBNM), Geel and the SCK-CEN, Mol to study the spontaneous fission of ^{240}Pu and the thermal neutron induced fission of ^{239}Pu by means of the so-called double energy method.

II. EXPERIMENTAL PROCEDURE

Preparatory measurements were performed at an 8 m flightpath of GELINA, the linear accelerator of the CBNM at Geel. Thermal neutrons were selected by time-of-flight out of the broad spectrum of moderated neutrons produced by GELINA. Spontaneous fission was measured during the weekends and the maintenance periods of GELINA. For these measurements, the same experimental arrangements as described in Ref. 9 were used. A mixed ^{239}Pu-^{240}Pu target (no. 1) on a transparent backing was mounted in the center of a vacuum chamber. The pulse-height spectra of coincident fission fragments were measured in a low geometry, with two collinear surface barrier detectors (area 6 cm^2), which were cooled at a constant temperature of 4 °C. These data pairs were binary coded and then stored on a magnetic tape unit via a Hewlett Packard 1000E computer. This computer was also used for the data reduction and analysis, which partially proceeded on-line.

The same apparatus was moved to a thermal neutron beam of the BR1 reactor of the SCK-CEN Nuclear Energy Center at Mol. This graphite moderated natural uranium reactor provides well-thermalized neutron beams with fluxes of about 10^6 neutrons/cm^2 sec. The reactor was operated only during the day and shutdown at night and during the weekends, which were almost ideal conditions for the present experiments. Indeed, such an operation allows one to measure a sequence of separate ^{240}Pu(sf)-^{239}Pu(n_{th},f) runs, which can be analyzed individually. So the spontaneous fission and the thermal fission measurements are alternated almost daily. Since the ^{239}Pu(n_{th},f) reaction is used for the detector calibration (cf. Sec. III), such a procedure allows a very careful followup of eventual variations in the calibration of the measuring chains. A careful calibration is indeed essential when studying highly α-radiating nuclei like ^{240}Pu (half-life 6550 yr) in view of the deterioration of the detector resolution caused by the radiation damage. This phenomenon has been studied, e.g., by Groh,[10] who concluded that an integrated dose of 3.4×10^{11} α's per detector should not be exceeded, since with such a dose the pulse-height defect about equals the energy resolution of the detector. Consequently, the total number of ^{240}Pu(sf) fragments correctly detected with a single detector is limited to about 17 000.

Two independent measurements were performed at the BR1 reactor: In the first one a very thin mixed ^{239}Pu-^{240}Pu target (no. 2) was used sandwiched between two 6

 ©1984 The American Physical Society

TABLE I. Target characteristics.

Target no.	Target thickness (μg Pu/cm^2)	Diameter (mm)	Backing thickness (μg polyimide/cm^2)	Gold coating (μg/cm^2)
1	58	20	30	
2	19	20	29	
3	57	30	30	21

cm^2 surface barrier detectors, resulting in an almost 4π detection geometry. This "sandwich" was mounted straight in the neutron beam, which was collimated to a diameter of 20 mm. In the second measurement a more classical low geometry configuration was used. Here a thicker mixed target (no. 3) was viewed by two collinear 20 cm^2 surface barrier detectors placed outside the neutron beam. Under these conditions, a total number of 25 000 coincident spontaneous fission fragments were recorded (15 000 in "4π" and 10 000 in low geometry).

The targets used were prepared by the CBNM Sample Preparation Group. A homogeneous mixture of 24% $^{239}PuF_3$ and 76% $^{240}PuF_3$ was evaporated onto very thin polyimide backings. With such a ^{239}Pu/^{240}Pu ratio, the ^{239}Pu(n$_{th}$,f) measurement is not influenced by the ^{240}Pu(sf) background. The detailed characteristics of the targets are summarized in Table I.

III. ANALYSIS

The analysis was based on the mass and momentum conservation relations and the Schmitt-Neiler[11] calibration procedure. The detector calibration constants[12] determined from the thermal neutron induced fission of ^{239}Pu were used to convert the measured pulse heights into energies. Using the ^{239}Pu(n$_{th}$,f) fission neutron emission data as a function of the fragment mass as obtained by Milton and Fraser,[13] the ^{239}Pu(n$_{th}$,f) preneutron emission fission fragment mass and energy distributions and mass-energy correlations were obtained via the iterative calculation described by Schmitt *et al.*[14] However, no fission neutron emission data as a function of the fragment mass are available for the spontaneous fission of ^{240}Pu. We therefore used the ^{239}Pu(n$_{th}$,f) fission neutron data of Milton and Fraser[13] multiplied by the ratio

$$\bar{\nu}[^{240}\mathrm{Pu(sf)}]/\bar{\nu}[^{239}\mathrm{Pu}(\mathrm{n_{th}},f)]$$

as given by Mughabghab and Garber.[15] This is a very acceptable approximation since it is well established that the shape of the $\nu(m^*)$ distribution is very similar for all fissioning isotopes.

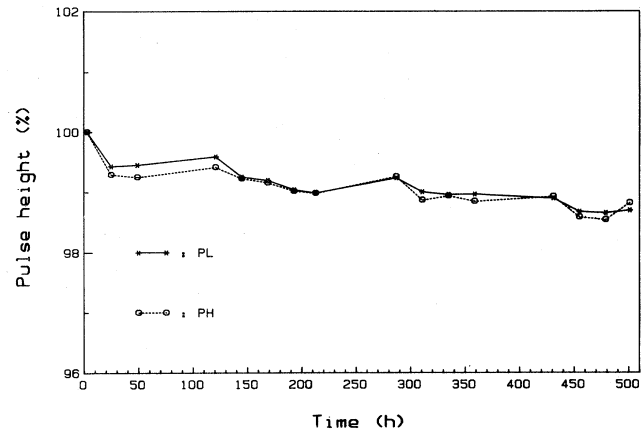

FIG. 1. Time dependency of the average light (PL) and heavy (PH) fragments pulse height for the ^{239}Pu(n$_{th}$,f) calibration runs during the low-geometry experiment.

Figure 1 shows the evolution of the average light and heavy fragments's pulse height for the ^{239}Pu(n$_{th}$,f) calibration runs during the low-geometry experiment. The small fluctuations around the linear decrease due to the radiation damage are of statistical nature and/or a consequence of the adjustments of the detector bias to compensate for the increased leakage current. In the measurements shown in Fig. 1, 15 ^{240}Pu(sf) runs have been performed. To make their calibration as accurate as possible, each of these runs has been analyzed separately with calibration constants determined from the ^{239}Pu(n$_{th}$,f) run preceding and following the spontaneous fission run. All these individual analyses were summed up afterwards. The same procedure was also followed for the "4π" geometry experiment.

TABLE II. Main characteristics of the ^{240}Pu(sf) and the ^{239}Pu(n$_{th}$,f) fragment mass and energy distributions. The errors are only statistical.

	Low geometry measurement		"4π" geometry measurement		
	^{239}Pu(n$_{th}$,f)	^{240}Pu(sf)	^{239}Pu(n$_{th}$,f)	^{240}Pu(sf)	^{240}Pu(sf) total
$\bar{E}_K$ (MeV)	175.38±0.01	177.04±0.12	175.40±0.01	177.44±0.10	177.28±0.08
$\bar{E}_K^*$ (MeV)	177.65±0.01	178.76±0.12	177.67±0.01	179.16±0.10	179.00±0.08
σE_K (MeV)	12.14	12.15	12.50	12.51	12.37
$\bar{E}_L^*$ (MeV)	103.29±0.01	103.18±0.09	103.32±0.01	103.43±0.07	103.33±0.06
$\bar{E}_H^*$ (MeV)	74.36±0.01	75.56±0.09	74.35±0.01	75.73±0.07	75.67±0.06
$\bar{m}_L^*$ (u)	100.30±0.01	101.32±0.06	100.27±0.01	101.31±0.05	101.31±0.04
$\sigma m_L^*=\sigma m_H^*$	6.64	5.74	6.63	5.74	5.74
$\bar{m}_H^*$ (u)	139.70±0.01	138.68±0.06	139.73±0.01	138.69±0.05	138.69±0.04
Peak yield (%)	6.08	7.57	6.01	7.49	7.52
Peak/valley (5 pts)	114 ±2	577 ±280	119 ±3	559 ±230	566 ±190
N	4.2×10^6	10^4	1.9×10^6	1.5×10^4	2.5×10^4

IV. RESULTS

As explained in the Introduction, the primary goal of the present experiments was to obtain an accurate comparison of the ^{240}Pu(sf) and the ^{239}Pu(n$_{th}$,f) mass and energy characteristics. The requested accuracy could be attained by using mixed ^{239}Pu-^{240}Pu targets, which strongly reduces the error on the intercomparison since the ^{239}Pu(n$_{th}$,f) and the ^{240}Pu(sf) fragments are emitted from *the same sample.*

In the following subsections we will report on the results of the measurements performed at the BR1 reactor, since these have the highest statistical accuracy. Within their lower statistical accuracy, the results of the measurement done at GELINA completely agree with the BR1 data.

A. Mass distributions

Table II summarizes the main characteristics of the ^{240}Pu(sf) and the ^{239}Pu(n$_{th}$,f) fragment energy and mass distributions obtained in the present work. This table clearly shows that the ^{240}Pu(sf) mass characteristics deduced from the low and the "4π" geometry measurements are in perfect agreement. The (preneutron emission) mass yield distributions for ^{240}Pu(sf) and ^{239}Pu(n$_{th}$,f) fragments are compared in Fig. 2. Both the table and the curves in the figure demonstrate a few striking differences between the (sf) and the (n$_{th}$,f) mass characteristics: The peak yield is higher, the width is smaller, and the peak-to-valley ratio is much larger in the ^{240}Pu(sf) case. For the same reaction, the average light and heavy fragment masses are shifted by 1 u towards symmetry compared to ^{239}Pu(n$_{th}$,f). Also the fine structure at masses ~ 135 and ~ 143 is more obvious for ^{240}Pu(sf). For the peak-to-valley ratio in the ^{240}Pu(sf) mass distribution we obtain a value of 566 ± 190, in agreement with the results of Thierens *et al.*[6] (400 ± 180) and Laidler and Brown[16] (≥ 270). This value is about five times larger than the corresponding value for ^{239}Pu(n$_{th}$,f), which illustrates again that the yield of symmetric fission fragments increases with increasing excitation energy.

TABLE III. Comparison of the experimental values for $\Delta\bar{E}^*_K = \bar{E}^*_K(\text{sf}) - \bar{E}^*_K(\text{n}_{th},f)$ for the spontaneous fission of ^{240}Pu and the thermal neutron induced fission of ^{239}Pu.

$\Delta\bar{E}^*_K$ (MeV)	Ref.
-1.5 ± 0.5	Mostovaya (Ref. 1)
$+3.7\pm2.1$	Toraskar and Melkonian (Ref. 2)
-1.1 ± 0.2	Deruytter and Wegener-Penning (Ref. 3)
$+0.7\pm0.4$	Basova *et al.* (Ref. 4)
-0.8 ± 0.3	Wagemans *et al.* (Ref. 5)
$+1.2\pm0.5$	Thierens *et al.* (Ref. 6)
-0.7 ± 0.3	Trochon (Ref. 7)
$+1.3\pm0.1$	This work

B. Kinetic energy distributions

Detailed characteristics of the energy distributions are summarized in Table II. In Fig. 3 the total kinetic energy distributions of the ^{239}Pu(n$_{th}$,f) and the ^{240}Pu(sf) fragments are compared. This figure illustrates the difference between both results: The total kinetic energy distribution for ^{239}Pu(n$_{th}$,f) is compatible with a Gaussian distribution, which is clearly not so in the spontaneous fission case. Moreover, the ^{240}Pu(sf) distribution is shifted towards higher kinetic energies, which is also reflected in the higher $\bar{E}^*_K$ values listed in Table II. Numerically, this results in a 1.3 ± 0.1 MeV higher average total kinetic energy for the ^{240}Pu(sf) reaction than for the ^{239}Pu(n$_{th}$,f) reaction. A survey of the experimental values obtained so far for this quantity is given in Table III. The present results are in agreement with those of Thierens *et al.*,[6] Basova *et al.*,[4] and Toraskar and Melkonian.[2] They con-

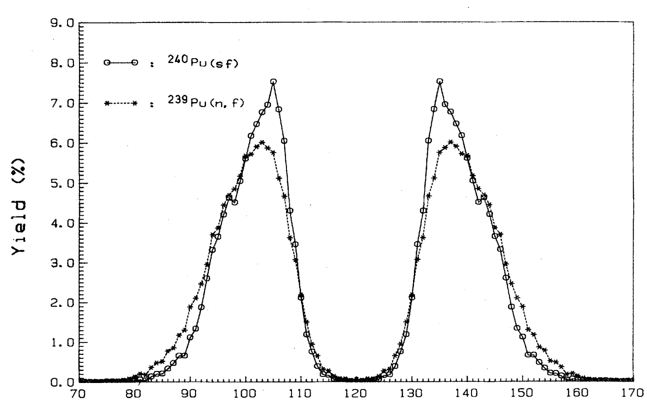

FIG. 2. Comparison of the (preneutron emission) mass yield distribution for the thermal neutron induced fission of ^{239}Pu (stars) and the spontaneous fission of ^{240}Pu (circles).

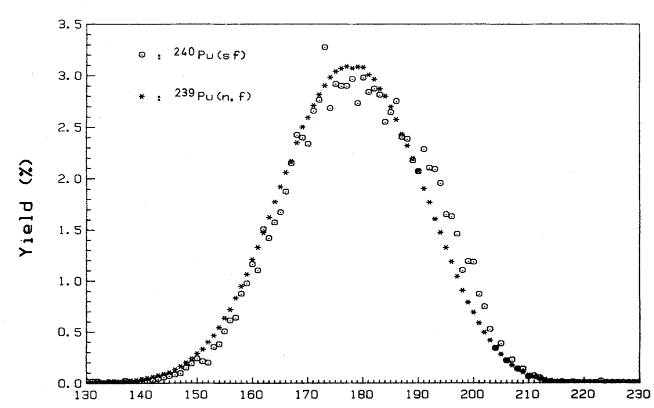

FIG. 3. Comparison of the total kinetic energy distribution ("4π" measurement) for the thermal neutron induced fission of ^{239}Pu (stars) and the spontaneous fission of ^{240}Pu (circles).

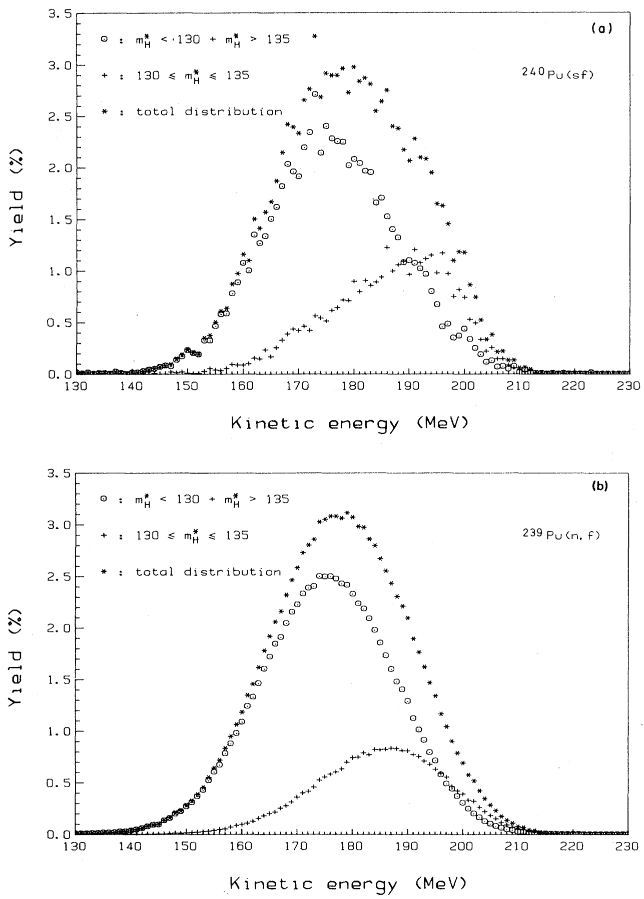

FIG. 4. Total kinetic energy distributions ("4π" measurement) for several mass intervals for the spontaneous fission of ^{240}Pu (a) and the thermal neutron induced fission of ^{239}Pu (b).

tradict our previous result[5] and those of Trochon,[7] Deruytter and Wegener-Penning,[3] and Mostovaya.[1] The important differences between the $\Delta\bar{E}_K^*$ values reported in Table III are probably a consequence of inaccuracies in the calibration procedure. As a consequence, some of the errors quoted (which, in most cases, are only statistical errors) might be underestimated. Furthermore, one should take into account that $\Delta\bar{E}_K^*$ is a rather small quantity corresponding only to 0.5%–1% of the measured $\bar{E}_K^*$ value.

C. Energy-mass correlations

In Fig. 4 the total kinetic energy distributions are split up into two parts, corresponding to the mass intervals $130 \le m_H^* \le 135$ (containing the doubly magic shell $N=82$, $Z=50$) and $120 \le m_H^* < 130$ plus $135 < m_H^* \le 174$. The average energies in both mass intervals are very different: 186.1 MeV for ^{240}Pu(sf) and 184.7 MeV for ^{239}Pu(n_{th},f) in the interval 130–135, compared to 176.0 MeV and 175.4 MeV, respectively, in the other interval.

In Fig. 5 the single fragment kinetic energy as a function of the fragment mass is shown for ^{240}Pu(sf) and ^{239}Pu(n_{th},f). These curves show the typical almost constant behavior for the light fragments, the dip in the symmetric mass region, and the strong decrease with increas-

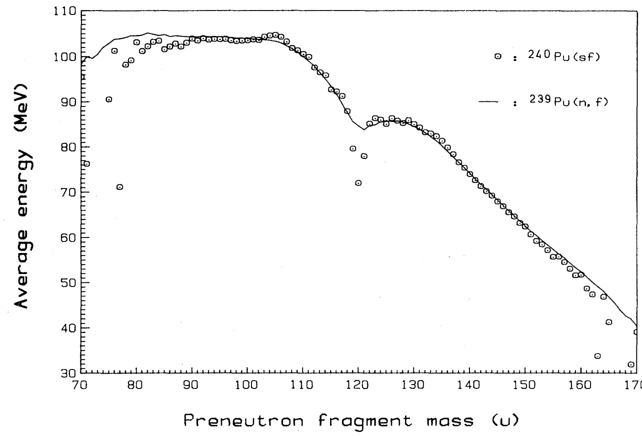

FIG. 5. The single fragment kinetic energy for the spontaneous fission of ^{240}Pu (circles) and the thermal neutron induced fission of ^{239}Pu (full line).

ing heavy fragment mass.

Figure 6 finally gives the $\bar{E}_K^*$ (m_H^*) curves with the typical maximum at mass ~ 132. Furthermore, the ^{239}Pu(n_{th},f) and the ^{240}Pu(sf) curves cross each other at $m_H^* \approx 140$.

V. DISCUSSION

The present results can be interpreted in terms of the nuclear shell effects presented in the scission point model of Wilkins *et al.*[17] The asymmetry of the total kinetic energy distribution for ^{240}Pu(sf) and, partly, also its higher $\bar{E}_K^*$ value, can be accounted for by the spherical $N=82$ shell. This shell will have its maximum influence for heavy fragments in the mass region 132–134, where the $N=82$ shell is enhanced by the $Z=50$ shell. This influence can be demonstrated[6] by a decomposition of the total fission fragment kinetic energy distribution for different mass splits. Figure 4(a) shows that the asymmetry in the total kinetic energy distribution for ^{240}Pu(sf) is mainly due to mass splits with $130 \le m_H^* \le 135$, for which the energy

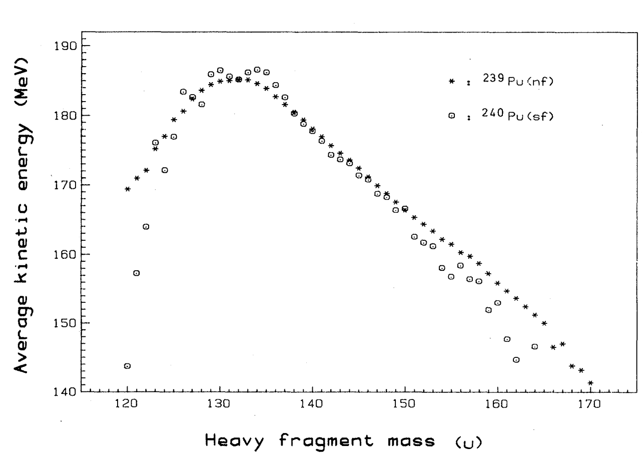

FIG. 6. Total fission fragment kinetic energy for ^{240}Pu(sf) (circles) and ^{239}Pu(n_{th},f) (stars) as a function of the heavy fragment mass.

distribution is strongly asymmetric. This is not so for the corresponding ^{239}Pu(n_{th},f) decomposite spectrum [Fig. 4(b)], which follows about a Gaussian distribution. Moreover, the corresponding average energy is about 1.4 MeV higher in the (sf) case. This can be understood in terms of the Wilkins model[6,17] by the preferential formation of an almost spherical ($\beta_1+\beta_2\approx0.95$) shell-stabilized configuration for mass splits with the heavy mass in the region of the closed neutron shell with $N=82$, compared to a second stable—but more deformed ($\beta_1+\beta_2\approx1.4$)—configuration in the same region, which is favored by a liquid drop behavior. The disappearance of the asymmetry in the energy distribution (which goes along with a lower average energy) for the thermal neutron induced fission of ^{239}Pu can be explained by a decrease of the shell corrections due to the 6.5 MeV increase of the excitation energy. This phenomenon can also be observed in Fig. 6, where the higher $\bar{E}_K^*$ (m_H^*) values for ^{240}Pu(sf) in the mass region 130—135 are also due to the nearly spherical shell-stabilized configuration with $N=82$. The same $N=82$ shell, enhanced by the deformed but stable $N=64$ shell in the light fragment, is also responsible for the enhanced yield in the ^{240}Pu(sf) mass distribution for masses around 132—134 (see Fig. 2). On the same curve, the enhanced yield in the heavy fragment mass region 142—144 can be explained by the combined influences of the broad deformed $N=88$ shell in the heavy fragment and the narrow $N=58$ shell in the light fragment.

The present results also yield information on the viscosity of the fissioning system ^{240}Pu. By combining the $\bar{E}_K^*$ values of Deruytter and Wegener-Penning[3] for ^{240}Pu(sf) with the isomeric fission data of Weber *et al.*[18] and their own ^{239}Pu(d,pf) results, Lachkar *et al.*[8] concluded that the fissioning system ^{240}Pu is superfluid below the fission barrier. So all the additional excitation energy is transformed into kinetic energy, resulting in a slope $d\bar{E}_K^*/dE_{exc}=+1$. This conclusion, however, was strongly influenced by the ^{240}Pu(sf) data, which are more than 2 MeV lower than the present value, which has been obtained under almost ideal conditions. In Fig. 7 the relevant $\bar{E}_K^*$ data for the fissioning system ^{240}Pu are plotted as a function of the excitation energy. Together with the present result for ^{240}Pu(sf), the isomeric fission value of Weber *et al.*,[18] the ^{239}Pu(d,pf) data of Lachkar *et al.*,[8] and the ^{239}Pu(n,f) data of Akimov *et al.*[19] are given. With these data, the slope $d\bar{E}_K^*/dE_{exc}$ is only $\sim+0.45$ below the barrier, indicating a strong damping of the fission mode.

One should, however, be very cautious when interpreting the data shown on Fig. 7. First, the data have been obtained in completely independent measurements, so absolute uncertainties have to be considered when intercomparing them. Second, one could wonder whether one should not make a distinction between the pure (liquid drop) damping of the fission mode and the shell effects. If we do such a calculation, e.g., for ^{240}Pu(sf) and ^{239}Pu(n_{th},f), we obtain that 1.6 MeV of the difference in $\bar{E}_K^*$ between both reactions is due to the difference in shell effects.

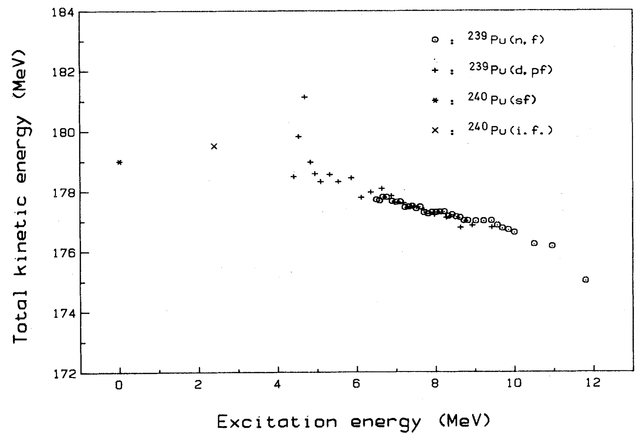

FIG. 7. Comparison of the present $\bar{E}_K^*$ value for ^{240}Pu(sf) (star) with the isomeric fission value of Weber *et al.* (Ref. 18) (cross), the ^{239}Pu(d,pf) data of Lachkar *et al.* (Ref. 8) (plus signs), and the ^{239}Pu(n,f) results of Akimov *et al.* (Ref. 19) (circles).

Anyhow, the present results make clear that for the fissioning system ^{240}Pu the fission mode below the barrier is damped and not superfluid as proposed by Lachkar *et al.*[8] This conclusion is in agreement with that of Thierens *et al.*[6] It is also endorsed by the very similar results which we obtained recently[9] for the fissioning system ^{242}Pu.

VI. CONCLUSION

In the present paper new and accurate results are reported on the ^{240}Pu(sf) fragment mass and energy characteristics, with a 25 000 events counting statistic. Striking differences between the ^{240}Pu(sf) and the ^{239}Pu(n_{th},f) characteristics could be explained in terms of the scission point model of Wilkins *et al.*,[17] and the damping of the fission mode below the barrier could be demonstrated.

ACKNOWLEDGMENTS

Special thanks are due to the CBNM Sample Preparation Group for the preparation of several high quality ^{239,240}Pu samples. Dr. C. Wagemans acknowledges the financial support by the Belgian National Fund for Scientific Research. This work was performed in the framework of a common research program between the CBNM, Geel, and the SCK-CEN, Mol, Belgium.

*Permanent address: SCK-CEN, Mol, Belgium and Nuclear Physics Laboratory, Gent, Belgium.

[1]T. Mostovaya, in *International Conference on Peaceful Uses of Atomic Energy, Geneva* (United Nations, New York, 1958), p. 2031.
[2]J. Toraskar and E. Melkonian, Phys. Rev. C **4**, 1391 (1971).
[3]A. Deruytter and G. Wegener-Penning, *Physics and Chemistry of Fission* (IAEA, Vienna, 1974), Vol. 2, p. 51.

[4]B. Basova *et al.*, IAEA Report INDC (CCP) 114/G, 1977.
[5]C. Wagemans, G. Wegener-Penning, H. Weigmann, and R. Barthélémy, *Physics and Chemistry of Fission* (IAEA, Vienna, 1980), Vol. 2, p. 143.
[6]H. Thierens, A. De Clercq, E. Jacobs, D. De Frenne, P. D'Hondt, P. De Gelder, and A. Deruytter, Phys. Rev. C **23**, 2104 (1981).
[7]J. Trochon, Report CEA-N-2214, 1981; and private communication.
[8]J. Lachkar, I. Patin, and J. Sigaud, J. Phys. (Paris) Lett. **36**, 79 (1975).
[9]E. Allaert, C. Wagemans, G. Wegener-Penning, A. Deruytter, and R. Barthélémy, Nucl. Phys. A **380**, 61 (1982).
[10]W. Groh, Diplomarbeit, Universität Giessen, 1979.
[11]H. Schmitt, W. Gibson, J. Neiler, F. Walter, and T. Thomson, *Physics and Chemistry of Fission* (IAEA, Vienna 1965), Vol. 1, p. 531.
[12]J. Neiler, F. Walter, and H. Schmitt, Phys. Rev. **149**, 894 (1966).
[13]J. Milton and J. Fraser, Annu. Rev. Nucl. Sci. **16**, 894 (1966).
[14]H. Schmitt, J. Neiler, and F. Walter, Phys. Rev. **141**, 1146 (1966).
[15]S. Mughabghab and D. Garber, Brookhaven National Laboratory Report BNL 325, 1973.
[16]J. Laidler and F. Brown, J. Inorg. Nucl. Chem. **24**, 1485 (1962).
[17]B. Wilkins, E. Steinberg, and R. Chasman, Phys. Rev. **14**, 1832 (1976).
[18]J. Weber, H. Specht, E. Konecny, and D. Heunemann, Nucl. Phys. A **221**, 414 (1974).
[19]N. Akimov, V. Vorobeva, N. Kabenin, N. Kolosov, B. Kurminov, A. Sergachev, L. Smirenkina, and M. Tarosko, Yad. Fiz. **13**, 484 (1971) [Sov. J. Nucl. Phys. **13**, 272 (1971)].